The Cochlear Implant

Bollengier Alexis
Faculty of Electrical Engineering
Email: alexis.bollengier@epfl.ch

Pajot Elias
Faculty of Microengineering
Email: elias.pajot@epfl.ch

Vrignaud Emma
Faculty of Neuro-X
Email: emma.vrignaud@epfl.ch

***Abstract*—In this paper we present an overview of the cochlear implant, a neural interface device that allows patients with hearing loss to perceive sound. We describe the limitations in spatial and temporal resolution that arise from the spread of neural excitation and from the temporal imprecision of conventional square pulses, and we present ramped current waveforms as a good alternative. Finally, we examine the evolution of neuromorphic analog filterbanks, discussing the architectural shift from early transconductance-based designs to modern log-domain silicon cochleae.**

I. Introduction

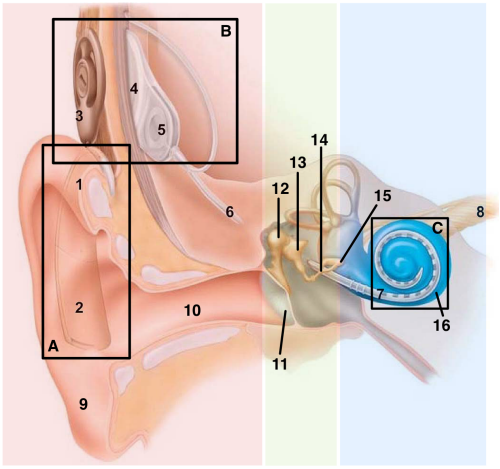

Fig. 1. Typical cochlear implant system that converts sound to electric impulses delivered to the auditory nerve and anatomy of the ear. [1].

A. The auditory pathway

The human ear is composed of three parts: the outer ear, the middle ear, and the inner ear, as shown in Fig. 1.

The outer ear (9) collects sound waves and channels them through the auditory canal (10) toward the eardrum (11).

The middle ear contains three small bones : the malleus (12), incus (13), and stapes (14), which transmit and amplify the vibrations of the eardrum. Malleus movement is transferred to the incus, which then moves the stapes. The stapes presses on the oval window (15), which is the gateway to the inner ear.

Inside the inner ear lies the cochlea (16), a spiral, snail-shell-shaped tube filled with fluid. When a mechanical wave (sound) travels through this tube, it causes movement of the basilar membrane, to which the hair cells are attached. This movement induces the bending of the stereocilia the cilia located at the apex of the hair cells. This bending generates an electrical potential that leads to a neural signal, which is transmitted to the brain via the auditory nerve (8), where they are interpreted as sound. [2]

B. Sound is encoded in multiple domains

In this context, sound is encoded both spatially and temporally: a given frequency at a certain amplitude at a certain moment. Spatial encoding follows the tonotopy. A sound of a certain frequency activates a specific region along the cochlear spiral, which stimulates the corresponding Spiral Ganglion Neurons (SGNs), which constitue the auditory nerve. In a hearing person, sound resolution is ensured by this fine-grained tonotopy and by the sharp mechanical and neural tuning of the cochlea. Temporal encoding corresponds to whether the signal is transmitted, how strongly it is transmitted, and when. In a hearing person, whenever a sound reaches the ear, SGNs fire reliably, roughly proportionally to amplitude, and with precise timing relative to acoustic events.

C. Sensorineural hearing loss and role of hair cells

Sensorineural hearing loss results from the irreversible deterioration of cochlear hair cells due to prolonged exposure to high sound levels or natural aging, as these cells do not regenerate. This deficit can be managed in two principal ways:

1) The least invasive solution is an external hearing aid, which simply amplifies sound.
2) If the hearing loss is severe or profound, rendering hearing aids ineffective, a cochlear implant is required.

D. The cochlear implant

The cochlear implant system is functionally divided into three principal components: the external unit (A), the coupling part (B), and the internal electrode array (C). (See Fig. 1) The external unit that powers all the implant by a battery (2), captures sound via a microphone (1). The acoustic signal is then digitized, processed (including bandpass filtering, spectral analysis, and compression), and encoded into a radio frequency (RF) signal. The RF signal is transmitted through an antenna in the headpiece (3), which is held in place by a magnet, to the internal receiver (4) implanted beneath the skin. The hermetically sealed stimulator (5) decodes the signal, converts it into electric currents, and sends them along wires (6) to the electrode array (7) threaded into the cochlea. These electrodes stimulate the auditory nerve (8) based on a precise

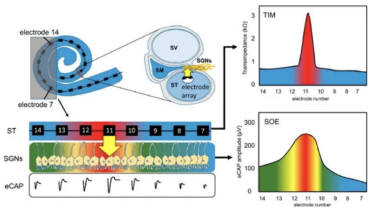

Fig. 2. This schematic highlights the principle of spread of neural excitation (SOE). Stimulation on electrode 11 spreads to neighboring cochlear regions, causing nearby SGNs to reach threshold and fire, resulting in overlapping excitation. [5]

frequency-to-place mapping, allowing the brain to interpret the impulses as sound [1].

Stimulation is commonly delivered using biphasic pulses, with a cathodic phase that depolarizes the neuron and an anodic phase to ensure charge balance.

II. Improvements in Resolution through Stimulation

With the Cochlear Implant being the oldest neural interface to exist, it is natural to wonder if there are any improvements left to be made or if researchers have plateaued. In fact, although the overall satisfaction is high [3], the CI's resolution remains limited, especially in noisy environments. CI users often report that they can follow speech in quiet rooms but struggle in noisy environments. In noise, speech and background sound activate overlapping neural populations with similar timing patterns, and the implant does not provide enough detail for the brain to differentiate the speech. This results in limited resolution.

A. Improving spatial and temporal resolution

In this context, resolution refers to how precisely the cochlear implant can represent the sound across two dimensions: which neurons along the cochlea are activated, and when they are activated. We can thus distinguish two types of resolution: spatial resolution and temporal resolution. Spatial resolution describes how selectively each electrode activates the intended region of SGNs, that is, how finely different frequencies are separated. Temporal resolution describes how reliably and precisely the timing of sound is encoded in the firing of these neurons. There has been a large focus on improving spatial resolution. It is difficult to increase the number of electrodes inside the cochlea because of its shape and size, so improvements include changing electrode placement and distribution, using more flexible arrays, or improving surgery with sensors [4]. These advances help reduce the spread of excitation and make stimulation more place-specific, but only to a point. Physical constraints and the conductive properties of the cochlear fluids mean that current spread is hard to limit just by changing the layout. Figure 2 shows how excitation spreads in the cochlea.

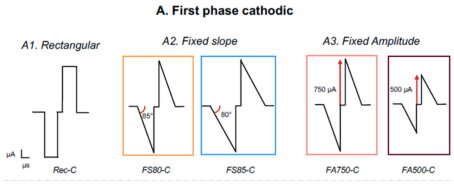

Fig. 3. Example of cathodic first current waveforms, used in *Partouche et al* which elicited higher temporal and spatial resolution

B. SGN particularities

As a reminder, potassium channels during an AP open gradually and eventually cause the hyperpolarization we observe. Spiral Ganglion Neurons have the particularity of expressing low-threshold voltage-gated potassium channels (often called KLT) [6]. These channels open with even small depolarizations. When KLT opens, potassium flows out of the cell, pushing the membrane potential back toward more negative values and opposing further depolarization. When the membrane becomes more negative again (hyperpolarized), these KLT channels close. In that state, they no longer oppose depolarization, and the neuron becomes more excitable: a subsequent depolarizing input can now more easily trigger an action potential.

C. New current waveform solution

There is another solution that can be deployed more readily in medical cochlear implants: using different current waveforms for stimulation. Through a better understanding of the target neurons, the Spiral Ganglion Neurons, it was suggested that stimulation waveforms with ramps (ascending or descending) could improve both temporal and spatial resolution [7] . In Figure 3, we observe a schematic of ramped waveforms, that are generated with a fixed angle or a fixed maximum amplitude

With standard square pulses, the abrupt onset and constant amplitude tend to produce broad, symmetric spread and strongly activate KLT channels. This can suppress or delay spikes and increase timing variability. A ramped current waveform exploits SGN physiology. The initial low-amplitude portion of the ramp produces a slowly changing depolarization that keeps KLT channels closed or allows them to deactivate, but only in neurons very close to the electrode. Distant neurons do not experience enough of this conditioning effect. As the ramp increases, the target neuron is "primed" and fires easily, while more distant neurons remain less excitable. This reduces spread and improves spatial resolution. Temporal resolution is facilitated because the membrane can reach threshold before KLT channels fully activate; sodium channels remain available, yielding reliable, precisely timed spikes. This is exactly what Partouche et al. observed: they noted a significantly increased spiking rate and lower thresholds needed for ramped stimulation, meaning that more pulses successfully produced spikes and at lower current levels. This suggests that with ramped waveforms we could increase spatial and temporal

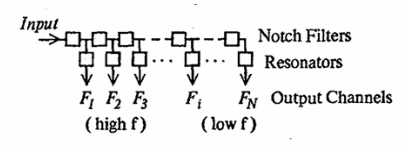

Fig. 4. Lyon's cascade-parallel cochlear model (1982) [8].

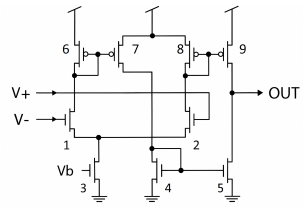

Fig. 5. The nine-transistor wide-range transconductance amplifier (OTA) [9].

resolution, and also reduce the power consumption of the implant.

III. CMOS Research Timeline

A. Foundations and First CMOS Implementation (1982 -1988)

A silicon cochlea is a neuromorphic chip that emulates how the biological cochlea analyzes sound. These devices are research models, not medical implants, but they provide valuable insight into cochlear filtering mechanisms and have inspired CIs. The development of silicon cochleae begins with Lyon's 1982 cascade-parallel filterbank model, illustrated in Fig. 4. The architecture reproduces the travel-wave behavior of the Basilar membrane through a sequence of second-order filters. Each filter has its center frequency decrease exponentially (due to weak inversion) from 20 kHz at the base to 50Hz at the apex. The structure is a 480-stage filter cascade, each stage controlled by two bias voltages that define the pole frequency and the quality factor ($Q \approx 0.79$). The Q factor is obtained by adjusting the theoretical second-order response until its resonance peak matches the measured AC response of the fabricated stage, as described in [9]. In this design, each 2^{nd} order filter is implemented as a gm-C section, where a transconductance (g_m) drives a capacitive load, and the pole frequency is set by the ratio g_m/C.

Figures 5 and 6 illustrate how this theoretical model is mapped onto CMOS circuitry. Figure 5 shows the schematic of the wide-range transconductance amplifier used in the cochlea chip implementation. The circuit operates in the weak inversion region and consists of a differential input pair (transistors 1 and 2) biased by a current source (transistor 3) set by voltage V_b. The differential currents are processed through two sets of current mirrors: the upper PMOS mirrors (transistors 6-7 and 8-9) and a bottom NMOS mirror (transistors 4-5), which converts the signal to a single-ended output. Unlike the basic five-transistor amplifier, this nine-transistor structure is designed to provide a wider range of output voltages and a higher DC voltage gain to behave as a follower as much as possible. Specifically, the output transistors (5 and 9) are

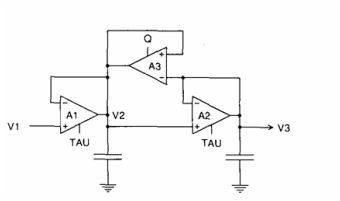

Fig. 6. The second-order filter section used in the 1988 analog cochlea. The circuit cascades two follower-integrators (A1, A2) to set the time constant τ, while amplifier A3 provides controlled positive feedback [9].

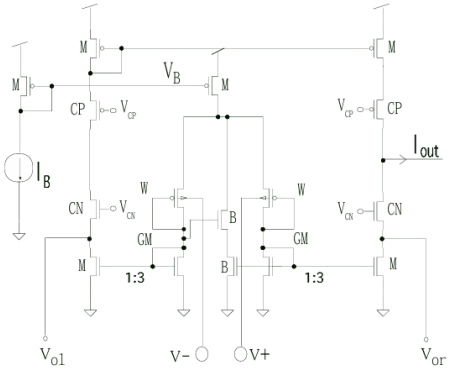

Fig. 7. Wide-linear-range transconductance amplifier used in Sarpeshkar's cochlea. [10]

designed with extra-long channel lengths to maximize output impedance, enabling high gain in the follower-integrator stages.

Fig. 6 shows how these OTAs combine into a second-order section implementing the travelling-wave filter of Fig. 4, with two integrators defining the time constant τ and a feedback amplifier (A3) setting the resonance peak and quality factor.

When mapped to CMOS, the approach shows several hardware limitations. The long 480-stage cascade amplifies noise accumulation, weak-inversion OTAs provide limited linearity and limit small-signal ranges. Neither in [8] nor in [9] level metrics such as device dimensions, noise floor, or dynamic range are mentioned, except for the reported resonance gain of 12 dB.

B. Noise and Dynamic-Range Breakthrough: The Sarpeshkar Cochlea (1998)

The 1998 analog cochlea by Sarpeshkar is the first fully measured cochlea that successfully overcomes the main limitations of the 1988 gm-C design. As shown in Fig. 8, each stage includes a second-order section whose pole frequency and quality factor are tuned by V_T and V_Q. This control is implemented using translinear biasing circuits, which provide Q-values that are approximately invariant with corner frequency and improve matching compared to 1988 CMOS designs.

A key feature of this enhancement is the wide-linear-range (WLR) OTA shown in Fig. 7. Unlike the 1988 OTA, which remained linear over only a few tens of millivolts, the 1998 amplifier maintains a stable and nearly linear g_m across an

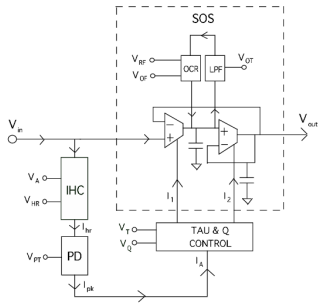

Fig. 8. Block-level schematic of a single cochlear stage in the 1998 analog VLSI cochlea [10].

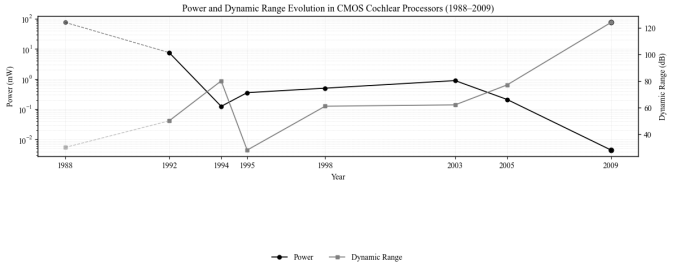

Fig. 9. Evolution of power consumption and dynamic range in CMOS cochlear implant (1988-2009).

input range on the order of volts. This wide-linear range is obtained through complementary mechanisms shown in Fig. 7: use of the wells of transistors (W) as input to lower g_m and then increase the linearity range, gate degeneration transistors (GM), which provide negative feedback to linearize the response, and bump-linearization elements (B), which extend linearity near zero-crossing ($V_+ = V_-$). In addition, cascode transistors (CP, CN) are employed to increase DC gain and prevent low-frequency attenuation [10].

The 1998 architecture resolves the noise-accumulation problem through a combination of offset adaptation and a novel overlapping cochlear cascades structure of 3 levels of 39 cascades to limit the accumulation of $1/f$ noise and group delay. Each stage prevents DC accumulation using local offset cancellation: a low-pass filter extracts the DC component, and the OCR block injects a correction current to restore the reference level V_{RF} to remove the offset. V_{RF} is the middle of the signal amplitude and must be such that the wave does not saturate to VDD or GND.

Dynamic range is enhanced by an Automatic Gain Control (AGC) loop. The Inner Hair Cell (IHC) and Peak Detector (PD) block generate a current I_{pk} proportional to the signal envelope. This current acts as a gain-control variable I_A that feeds into the bias circuit to lower the (Q) for large signals. By dynamically attenuating Q at high amplitudes to avoid distortion while maintaining high sensitivity for small signals, as explained in detail in [10].

These improvements translate into a measurable dynamic range of 61 dB at 4 % THD[1], with a total static power consumption of only 0.5 mW for a $31.28mm^2$ size.

C. State-of-the-Art Log-Domain Cochlea: The Katsiamis Architecture (2009)

The 2009 cochlea by Katsiamis introduces a log-domain and Class-AB architecture that differs completely from the gm-C approach used in past systems. By operating in the log domain, the circuit exploits the exponential $I - V$ characteristics of MOS transistors in weak inversion to implement companding (compression and expansion), allowing large input dynamic range to be processed with small voltage swings. Class-AB biasing ensures that current is drawn only when required by the signal, which reduces the power consumption while maintaining sufficient linearity for filter operation.

The AGC mechanism acts in feed-forward to dynamically adapt the Quality Factor of the filter stages according to the input signal amplitude. Unlike the 1998 architecture, which relied on a long cascade (3×39 stages) requiring offset adaptation, this design utilizes a short-cascade channel architecture. This structure change prevents the noise and offset accumulation, reducing the need for extensive stage-by-stage correction. This system is covered in detail in [11].

These architectural choices lead to measurable performance improvements. The 2009 cochlea achieves a dynamic range of 124 dB with a static power consumption of 4.46 μW for $2.25mm^2$ size, compared with the 61 dB dynamic range and 0.5 mW consumption reported for the 1998 design.

D. Metrics Analysis

Figure 9 summarizes the evolution of power consumption and dynamic range across CMOS cochlear processors from 1988 to 2009. The trend is clear: dynamic range steadily increases while power decreases by several orders of magnitude. This improvement is largely driven by advancements in CMOS technology scaling, which reduces device dimensions, lowers parasitic capacitances, and allows bias currents to be significantly minimized. [12]

IV. Conclusion

Cochlear implants are the oldest modern neural interface, but there is still a long way to go in improving their resolution. Multiple solutions are being explored, and the next major advance could be ramped waveforms, which are easier to implement medically than hardware modifications. It is also important to consider the theoretical models and reflections that support such improvements, silicon cochlea. Over the years, CMOS cochlear designs have steadily improved in efficiency, size, and power consumption, while supporting dynamic ranges that exceed those of the human auditory system. The evolution from simple OTA-based cascades to log-domain frequency processing has significantly increased accuracy and robustness, making modern CMOS architectures suitable for long-term, wearable implantable devices.

[1]THD: ratio of distortion harmonics to the fundamental

REFERENCES

[1] F.-G. Zeng, S. Rebscher, W. Harrison, X. Sun, and H. Feng, "Cochlear implants: System design, integration, and evaluation," *IEEE Reviews in Biomedical Engineering*, vol. 1, p. 118, November 2008.

[2] D. Fitzpatrick, "Cochlear implants," in *Implantable Electronic Medical Devices*. Elsevier, 2015, ch. 5, pp. 53–56.

[3] C. C. Wick, D. Kallogjeri, J. L. McJunkin, N. Durakovic, L. K. Holden, J. A. Herzog, J. B. Firszt, and C. A. Buchman, "Hearing and quality-of-life outcomes after cochlear implantation in adult hearing aid users 65 years or older," *JAMA Otolaryngology–Head & Neck Surgery*, vol. 146, no. 10, p. 925, 2020.

[4] Y. N. Ertas, D. Ozpolat, S. N. Karasu, and N. Ashammakhi, "Recent advances in cochlear implant electrode array design parameters," *Micromachines*, vol. 13, no. 7, p. 1081, 2022.

[5] S. Söderqvist, S. Lamminmäki, A. Aarnisalo, T. Hirvonen, S. T. Sinkkonen, and V. Sivonen, "Intraoperative transimpedance and spread of excitation profile correlations with a lateral-wall cochlear implant electrode array," *Hearing Research*, vol. 405, p. 108235, 2021.

[6] Y. Lu, P. Monsivais, B. L. Tempel, and E. W. Rubel, "Activity-dependent regulation of the potassium channel subunits kv1.1 and kv3.1," *Journal of Comparative Neurology*, vol. 470, pp. 93–106, 2004.

[7] E. Partouche, V. Adenis, P. Stahl, C. Huetz, and J.-M. Edeline, "What is the benefit of ramped pulse shapes for activating auditory cortex neurons? an electrophysiological study in an animal model of cochlear implant," *Brain Sciences*, vol. 13, no. 2, p. 250, 2023.

[8] R. F. Lyon, "A computational model of filtering, detection, and compression in the cochlea," in *Proc. IEEE International Conference on Acoustics, Speech, and Signal Processing (ICASSP)*. Paris, France: IEEE, 1982, pp. 1282–1285.

[9] R. F. Lyon and C. Mead, "An analog electronic cochlea," *IEEE Transactions on Acoustics, Speech, and Signal Processing*, vol. 36, no. 7, pp. 1119–1134, July 1988.

[10] R. Sarpeshkar, R. F. Lyon, and C. Mead, "A low-power wide-dynamic-range analog vlsi cochlea," *Analog Integrated Circuits and Signal Processing*, vol. 16, no. 3, pp. 245–274, 1998.

[11] A. G. Katsiamis, E. M. Drakakis, and R. F. Lyon, "A biomimetic, 4.5 μw, 120+db, log-domain cochlea channel with agc," *IEEE Journal of Solid-State Circuits*, vol. 44, pp. 1006–1022, 2009.

[12] A. Katsiamis and E. M. Drakakis, "Analogue cmos cochlea systems: A historic retrospective," in *Biomimetic Based Applications*, M. Cavrak, Ed. InTech, 2011, ch. 16, pp. 429–472.